Energy-Linked Binding of P_i Is Required for Continuous Steady-State Proton-Translocating ATP Hydrolysis Catalyzed by F_o·F_1 ATP Synthase†

Tatyana V. Zharova and Andrei D. Vinogradov*

Department of Biochemistry, School of Biology, Moscow State University, Moscow 119992, Russian Federation

Received July 28, 2006; Revised Manuscript Received September 28, 2006

ABSTRACT: The presence of medium P_i (half-maximal concentration of 20 μM at pH 8.0) was found to be required for the prevention of the rapid decline in the rate of proton-motive force (pmf)-induced ATP hydrolysis by F_o·F_1 ATP synthase in coupled vesicles derived from *Paracoccus denitrificans*. The initial rate of the reaction was independent of P_i. The apparent affinity of P_i for its "ATPase-protecting" site was strongly decreased with partial uncoupling of the vesicles. P_i did not reactivate ATPase when added after complete time-dependent deactivation during the enzyme turnover. Arsenate and sulfate, which was shown to compete with P_i when F_o·F_1 catalyzed oxidative phosphorylation, substituted for P_i as the protectors of ATPase against the turnover-dependent deactivation. Under conditions where the enzyme turnover was not permitted (no ATP was present), P_i was not required for the pmf-induced activation of ATPase, whereas the presence of medium P_i (or sulfate) delayed the spontaneous deactivation of the enzyme which was induced by the membrane de-energization. The data are interpreted to suggest that coupled and uncoupled ATP hydrolysis catalyzed by F_o·F_1 ATP synthases proceeds via different intermediates. P_i dissociates after ADP if the coupling membrane is energized (no E·ADP intermediate exists). P_i dissociates before ADP during uncoupled ATP hydrolysis, leaving the E·ADP intermediate which is transformed into the inactive ADP(Mg^{2+})-inhibited form of the enzyme (latent ATPase).

F_o·F_1 synthases (ATPases) catalyze the production of ATP from ADP and P_i at the expense of the transmembrane proton (Na^+)-motive force (pmf),[1] generated by electron transfer reactions in the respiratory chains of mitochondria, chloroplasts, and bacterial plasma membranes. They are also capable of pmf generation with the use of energy from ATP hydrolysis; thus, the F_o·F_1 complex phenomenologically operates as the reversible energy-transducing device. The integral structures of F_o·F_1's in all species studied so far are remarkably similar (*1*−*4*). The structures (*5*, *6*), as related to rotary binding change mechanism (*7*−*10*) and kinetic properties (*11*) of F_1-type ATPases, have been extensively discussed.

When assayed either in the presence or in the absence of the ATP-regenerating system, F_1 and F_o·F_1 ATPases exhibit complex time-dependent kinetics that are due to the relatively slow (as compared with the enzyme turnover) formation of the so-called ADP(Mg^{2+})-deactivated form, the phenomenon characteristic for all F_1-type ATPases that have been studied. The fractional population of the ADP(Mg^{2+})-inhibited form in a certain preparation of F_1 ATPase depends on a number of factors, such as the ATP/ADP ratio, pmf, free Mg^{2+} and inorganic phosphate concentrations, and the particular source of the enzyme (reviewed in ref *11*). The most intriguing property of the ADP(Mg^{2+})-deactivated ATPase is that being inactive in ATP hydrolysis, it is fully competent in the ATP synthase activity (*12*, *13*).

Evidence that F_o·F_1 operates in the specific "hydrolase" or "synthase" modes depending on the presence of ATP, ADP, and pmf has been gradually accumulating (*12*−*16*). To create a model describing the reaction pathways in either the hydrolytic or synthetic direction of catalysis, quantitative information about interactions of the substrates (products), ATP, ADP, P_i, and Mg^{2+}, with the enzyme is required. Numerous important studies of the nucleotide binding properties of F_1 from different sources have been published and reviewed (see ref *17* and references cited therein). Less attention has been paid to P_i as the product (substrate) of ATP hydrolysis (synthesis), although its binding properties seem equally important for the understanding of the F_o·F_1 operation mechanism. Recently, we have shown that the presence of P_i in the assay mixture is required for the steady-state ATP hydrolysis catalyzed by tightly coupled vesicles derived from *Paracoccus denitrificans* plasma membrane (*18*). This paper describes further analysis of this phenomenon. To our knowledge, multiple effects of P_i on F_1-type ATPases which may or may not be directly related to the mechanism of ATP synthesis have never been reviewed, and a brief account of the available data on this topic as outlined below seems to be appropriate for the introduction.

Soluble bovine heart and *Escherichia coli* F_1's bind more than 1 mol of P_i per mole of enzyme with an apparent affinity

† This work was supported by the Russian Foundation for the Fundamental Studies (Grant 05-04-48809 to A.D.V.).

* To whom correspondence should be addressed. Telephone and fax: 7-(495)-939-1376. E-mail: adv@biochem.bio.msu.su.

[1] Abbreviations: CCCP, carbonyl cyanide 3-chlorophenylhydrozone; CF_o·F_1, EF_o·F_1, MF_o·F_1 PF_o·F_1, and TF_o·F_1, ATP synthase complexes in chloroplasts, *Escherichia coli*, bovine heart mitochondria, *Paracoccus denitrificans*, and thermophilic *Bacillus* PS3, respectively; NBD-Cl, 7-chloro-4-nitrobenzofurazan; pmf ($\Delta\tilde{\mu}_{H^+}$), difference between the electrochemical potential of the hydrogen ion at different sides of the coupling membrane.

10.1021/bi061520v CCC: $33.50
Published on Web 11/04/2006

in the micromolar range (*19*−*21*). Sulfate, sulfite, and chromate enhance P_i binding, whereas efrapeptin and azide, the specific inhibitors of ATP hydrolysis, inhibit P_i binding (*19*, *20*). The removal of tightly bound nucleotides from MF_1 prevents P_i binding, which is restored by preincubation of the enzyme with purine nucleotides (*22*). P_i bound to F_1 is displaced by medium phosphate (*19*). Both the binding of P_i to and the dissociation of P_i from MF_1 are slow processes that proceed on a minute time scale (*19*). The slow displacement of bound P_i is, however, greatly accelerated by ATP or ADP (*23*). Under the unisite ATP hydrolysis ($[MF_1] \geq [ATP]$), the first-order rate constant for P_i and ADP release has been estimated to be 4×10^{-3} s^{-1} (*24*, *25*). P_i ($K_a \sim 1$ mM) was shown to stimulate the energy-promoted hydrolysis of ATP bound at a single high-affinity ($K_a \sim 10^{12}$ M^{-1}) catalytic site of F_o·F_1 in coupled submitochondrial particles (*26*).

Variable K_m's for F_o·F_1-catalyzed synthesis of ATP have been reported in the literature. These are 0.5−6 mM for MF_o·F_1 (*27*−*31*), 0.6−3.5 mM for EF_o·F_1 (*32*−*34*), 10 mM for TF_o·F_1 (*35*), 0.25 mM for CF_o·F_1 (*36*), and 0.15−0.35 mM for PF_o·F_1 (*37*−*39*). The apparent affinity of F_o·F_1 for P_i in oxidative phosphorylation was shown to dependent on the rate of respiration and/or the steady-state magnitude of pmf (*27*, *29*, *30*, *33*, *37*, *39*). An order of the substrates binding to F_1 during ATP synthesis, if the same for different species, remains uncertain. Evidence for both ordered (*31*, *40*) and random (*38*, *39*) kinetic mechanisms has been published. Kayalar et al. (*41*) and Perez and Ferguson (*38*) have suggested a randomly ordered bi-uni reaction catalyzed by MF_o·F_1 and PF_o·F_1, respectively, whereas the compulsory ordered mechanisms where P_i binds first [MF_o·F_1 (*31*)] or ADP binds first [CF_o·F_1 (*40*)] have been suggested for oxidative and photophosphorylation, respectively.

The fact that the exchange of medium P_i with $H_2{}^{18}O$ catalyzed by coupled submitochondrial particles in the presence of ATP and ADP is as sensitive to uncoupling as [^{32}P]ATP exchange and net oxidative phosphorylation, whereas during uncoupled ATP hydrolysis, each P_i that is released contains more than one water ^{18}O (intermediate exchange), was interpreted as evidence of the requirement of energy for binding of P_i to the catalytic site where the reversible energy-independent ATP formation takes place (*42*). The energy-independent enzyme-bound ATP formation from medium P_i has been directly demonstrated for CF_1 (*43*), CF_o·F_1 (*44*), MF_1 (*45*), and TF_1 (*46*). The half-maximal concentration of P_i required for this reaction was in the range of 20−40 mM.

P_i was shown to increase the ATPase activity of rat liver mitochondria (*47*), submitochondrial particles derived therefrom (*48*, *49*), or bovine heart soluble F_1 (*49*) at 1−20 mM. This phenomenon is apparently due to the antagonistic effect of P_i on ADP(Mg^{2+})-induced deactivation of F_1 or F_o·F_1 (*50*, *51*). Indeed, P_i decreases the extent of high-affinity ADP-specific inhibitory binding in submitochondrial particles by 2 orders of magnitude (7×10^{-8} and 5×10^{-6} M in the absence and presence of 10 mM P_i, respectively) (*50*). P_i ($K_d = 1$ mM) also increases the rate of activation of the ADP-inhibited MF_o·F_1 in the absence of free Mg^{2+} (*51*). The α-subunit "noncatalytic" site-deficient TF_1 $\alpha_3\beta_3\gamma$ complex and F_o·F_1 reconstituted from this complex are incapable of ATP hydrolysis because of instant entrapment of ADP in their tight inhibitory site (*14*, *52*). These mutant enzymes, however, catalyze continuous ATP hydrolysis in the presence of high (maximal rate at 150 mM) P_i concentrations (*53*). The trypsin cleavage of the ϵ-subunit of EF_1 in the presence of ADP and Mg^{2+} was protected by P_i at the half-maximal concentration of 50 μM (*54*). P_i was also shown to protect ATPase in submitochondrial particles against irreversible inactivation by NBD-Cl at half-maximal efficiency reached at 0.2 mM (*55*). Recently, the "coupling" effect of P_i (along with ADP) at relatively low concentrations (half-maximal at 30 μM) on the proton translocating activity of F_o·F_1 ATPase in *Rhodobacter capsulatus* chromatophores has been described (*56*).

Coupled plasma membrane vesicles derived from *P. denitrificans* do not catalyze ATP hydrolysis unless they are exposed to respiration-induced pmf (*18*, *57*). As noted above, the presence of medium P_i was found to be indispensable for the pmf-induced proton-translocating ATP hydrolysis catalyzed by PF_o·F_1 (*18*). Here we have examined the dependence of coupled ATPase on P_i. The data show that energy-dependent high-affinity P_i-binding site(s) must be occupied by P_i or by other anions (arsenate and sulfate) during the steady-state proton-translocating ATP hydrolysis to prevent the ADP(Mg^{2+})-induced inhibition of the enzyme. The minimal kinetic scheme describing coupled and uncoupled ATP hydrolysis catalyzed by F_o·F_1 ATP synthases is proposed and discussed with regard to the mechanism and reversibility of ATP hydrolysis.

MATERIALS AND METHODS

P. denitrificans (strain 1222) plasma membrane vesicles were prepared from a culture grown in the presence of succinate and nitrate (*58*). Under optimal conditions (*57*), the vesicles catalyzed the pmf-activated proton-translocating ATPase reaction [150 nmol min^{-1} (mg of protein)$^{-1}$] and succinate-supported ATP synthesis [300 nmol min^{-1} (mg of protein)$^{-1}$] at 30 °C. ATP hydrolysis and ATP synthesis were more than 90% sensitive to venturicidin and uncoupler, respectively. The rates of ATP hydrolysis or ATP synthesis were measured as small pH changes followed by Phenol Red responses (*59*). The level of inorganic phosphate was determined as described in ref *60*. The standard reaction mixture for the ATPase assay was comprised of 0.25 M sucrose, 0.1 M KCl, 2.5 mM Hepes, 0.1 mM EDTA, 5.5 mM $MgCl_2$, 2.5 mM succinate, 20 mM malonate, 2 mM ATP (potassium salts, pH 8.0), and 25 μM Phenol Red. ATP synthesis was assessed in the standard reaction mixture (except malonate was absent) supplemented with inorganic phosphate and ADP. The transmembrane potential was followed as Oxonol VI (1.5 μM) response at 624−602 nm. Oxygen consumption was assessed amperometrically with a platinum-coated oxygen-sensitive electrode. Other experimental details were described in our previous paper (*18*) or are given in the figure legends. Protein content was determined by the biuret procedure with bovine serum albumin as a standard. All fine chemicals were from Sigma, while other reagents were of the highest purity available from local suppliers.

RESULTS

The following background is relevant to the results on the steady-state pmf-induced ATPase activity of PF_o·F_1. It has

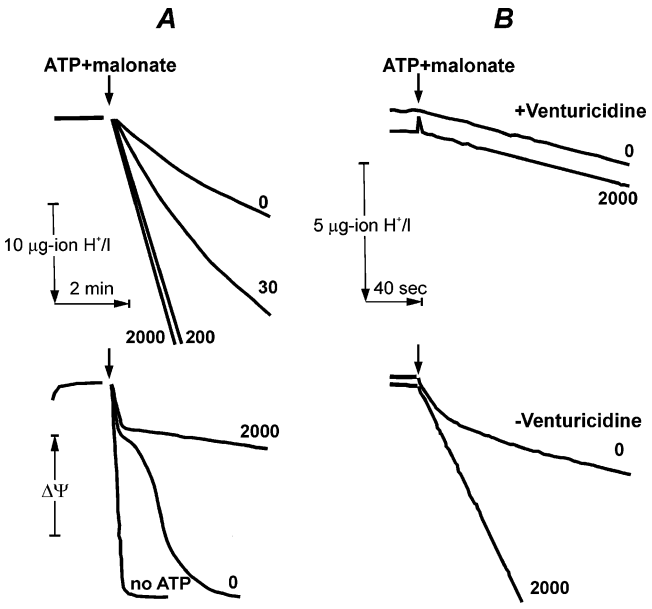

FIGURE 1: Effect of medium P_i on the time course of ATP hydrolysis. The vesicles (65 μg/mL) were added to the standard reaction mixture containing no malonate. After incubation for 2 min (coupled pmf-generating respiration), ATP hydrolysis was initiated by simultaneous addition of 1 mM ATP and 20 mM malonate (to eliminate succinate oxidation). (A) ATP hydrolysis (top panel, Phenol Red response) and membrane energization (bottom panel, Oxonol VI response) were followed in the standard reaction mixture containing P_i at the micromolar concentrations given on the curves. (B) Initial rate tracing of ATPase at higher sensitivity and time resolution. To ensure that the initial burst of Phenol Red response is, indeed, due to ATP hydrolysis, the control tracings where the vesicles were preincubated for 30 min with venturicidin, the specific inhibitor of prokaryotic ATPase (2 μg/mg of protein), are shown (top curves).

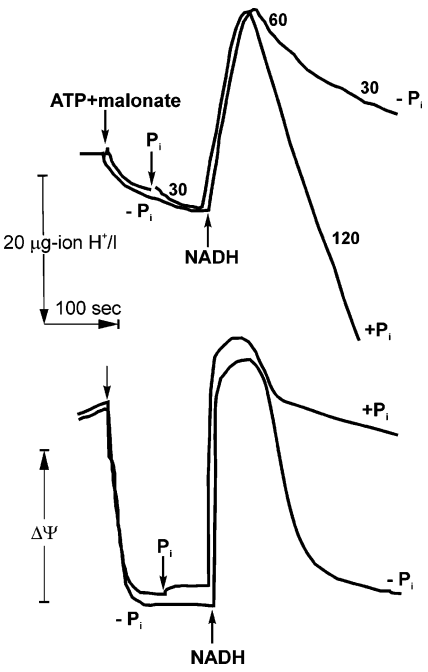

FIGURE 2: P_i is unable to reactivate ATPase that is deactivated during ATP hydrolysis in the absence of P_i. ATP hydrolysis (top panel, Phenol Red response) and membrane energization (bottom panel, Oxonol VI response) were followed in the standard reaction mixture containing vesicles (73 μg/mL). After ATPase activity has declined (in the absence of P_i), 2 mM P_i was added where indicated followed by the addition of 35 μM NADH. Oxidation of NADH by the respiratory chain was accompanied by alkalinization of the medium according to the stoichiometric equation $NADH + H^+ + {}^1/_2O_2 \rightarrow NAD^+ + H_2O$, which was evident from the Phenol Red response (top panel) and transitory membrane energization (bottom panel). In the control experiments (not shown), NADH oxidation followed by the change in absorption at 340 nm was found to be synchronous with alkalinization of the medium followed by Phenol Red response. Neither ATPase activity nor the membrane energization was affected by the addition of NADH to the assay medium originally containing 2 mM P_i. The specific ATPase activities (nanomoles per minute per milligram of protein) are indicated by the numbers on the curves (top panel).

been shown that venturicidin-sensitive ATP hydrolytic activity of the vesicles as prepared is negligible unless pmf across the membrane is created by coupled oxidation of the respiratory substrate (succinate) (*18*). The proton-translocating ATP hydrolysis can then be seen if succinate oxidation is prevented by malonate. The ATPase activity thus revealed is stimulated by mild uncoupling (slight increase in the vectorial H^+ cycling rate) and is inhibited if the membrane permeability for protons is sufficiently high to collapse pmf. The continuous steady-state ATPase activity is thus self-supporting: pmf generated by $F_o{\cdot}F_1$ ATPase is used to maintain the enzyme in its catalytically competent state. One should realize that any influence which decreases the rate of enzyme turnover is expected to cause two effects: a decrease in the overall enzyme activity and, as a result, a decrease in the fraction of active enzyme due to pmf reduction. Figure 1A shows the actual tracing of ATP hydrolysis and the membrane energization when the enzyme assays were conducted in the presence of different concentrations of P_i.

ATP hydrolysis coupled with pmf generation was not seen in the absence of P_i in the assay, whereas zero-order ATPase and significant pmf generation, evident from the steady-state Oxonol response, proceeded in the presence of 2 mM P_i. Only transitory maintenance of pmf and a time-dependent decrease in the ATPase activity which was synchronous with a decrease in the magnitude of the Oxonol VI response were observed in the absence of P_i. The results shown in Figure 1A prompted us to follow the rate of the ATPase reaction at higher sensitive and time resolution. As seen in the traces shown in Figure 1B, the absence of ATPase activity in the samples containing no P_i was only apparent: the initial rates of ATP hydrolysis were independent of P_i, and a rapid decline of ATPase was seen in the absence of P_i. Determining whether the rapid deactivation of ATPase seen in the absence of P_i could be reversed was worth investigating. Figure 2 shows that the addition of 2 mM P_i (the concentration which is sufficient to support continuous zero-order proton-translocating ATP hydrolysis as depicted in Figure 1A) after the activity had declined did not induce ATPase activity. However, the activity was fully restored if the membranes were energized (as seen from the Oxonol VI response) by oxidation of a limited amount of NADH. After NADH has been consumed, rapid zero-order ATP hydrolysis was observed.

Next we investigated the pmf dependence of the protecting effect of P_i against the enzyme deactivation. The time-dependent ATPase activity measured at a fixed time (20 s) after initiation of the reaction by simultaneous addition of ATP and malonate was plotted as a function of P_i concentration in the assay mixture containing various concentrations of protonophoric uncoupler (CCCP) (Figure 3).

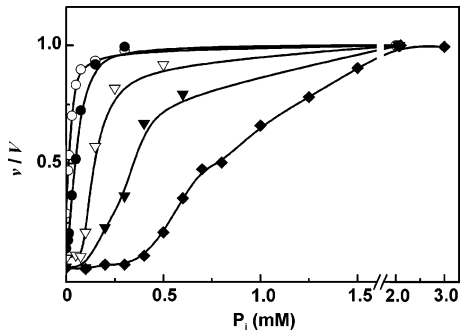

FIGURE 3: Effect of mild uncoupling on the protection of ATPase against deactivation by P_i. ATP hydrolysis was followed in the standard reaction mixture [containing vesicles (65 μg/mL)] and supplemented with P_i (concentrations are indicated on the abscissa). The specific ATPase activities (v) were estimated from the slopes of the reaction course curves 20 s after the reaction was initiated by the addition of ATP, malonate, and CCCP (simultaneously) as in Figure 1: (○) 0, (●) 0.3, (▽) 1.0, (▼) 2.0, and (◆) 3.0 μM uncoupler. The specific initial rates (V) were stimulated upon uncoupling, and apparent rates estimated 20 s after time zero were normalized (v/V), where V corresponds to the rates seen at given uncoupler concentrations in the presence of 2 mM P_i. Please note that true initial rates were P_i-independent as shown in Figure 1.

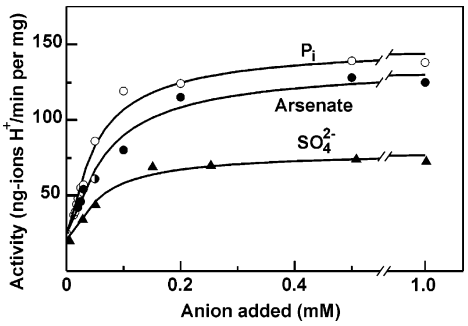

FIGURE 4: Arsenate and sulfate substitute for P_i in the protecting effect against the turnover-dependent deactivation of ATPase. The experimental conditions were the same as those described in the legend of Figure 3, except the uncoupler was not added.

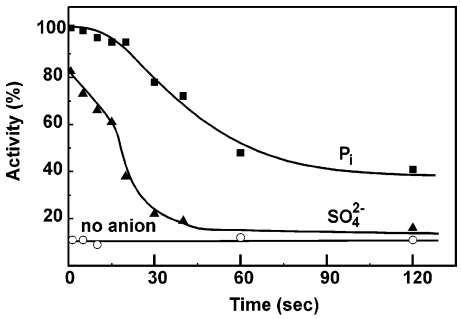

FIGURE 5: Protective effect of P_i and sulfate on spontaneous deactivation of ATPase after de-energization of the membranes. Vesicles (80 μg/mL) were preincubated in the standard assay mixture containing no malonate for 2 min (energization of the membranes). Malonate (20 mM) was then added, and ATP hydrolysis was initiated by the addition of 2 mM ATP at the time indicated on the abscissa. The initial rates were measured as described in the legend of Figure 1A. P_i (2 mM) or sulfate (2 mM) was added to the assay medium where indicated. The circles depict data from the case in which no protecting anion was added. P_i and sulfate did not affect pmf-induced activation of ATPase. One hundred percent corresponds to a specific activity of 150 nmol min^{-1} (mg of protein)$^{-1}$.

Although this approach is not quantitative, the results that were obtained clearly show that the apparent affinity of P_i for its ATPase "protecting" site is pmf-dependent. The half-maximal concentration of P_i ($P_{i,0.5}$) required for full ATPase activity was 15 μM and drastically increased upon partial uncoupling. It was noted that $P_{i,0.5}$ was variable depending on the coupling efficiency for different batches of the vesicle preparations. In attempts to clarify the variability of $P_{i,0.5}$ values, various ATPase assay media were tested. Surprisingly, no P_i requirement for the continuous zero-order ATP hydrolysis was found at all when KCl was omitted from the standard mixture. Further inspection revealed that the assay mixture (with or without KCl) contained 10 μM P_i as contamination from the vesicles (17 nmol/mg) and from potassium hydroxide used for the pH adjustment. In a KCl-free assay mixture, this concomitant P_i (10 μM) was sufficient to protect ATPase against deactivation. From the data shown in Figure 3 and described above, it became evident that the energy-dependent high-affinity P_i binding is required to protect PF_o·F_1 ATPase against the deactivation. This conclusion was corroborated by the partial uncoupling effect of potassium chloride: the respiratory control ratio determined with NADH as the substrate was 4.2 and 3.3 in the absence and presence of 0.1 M KCl, respectively. These results agree with those of Kell et al. (*61*), who have reported that the presence of KCl decreased the pmf of *P. denitrificans* vesicles respiring with NADH from 150 to 115 mV.

Next, the specificity of P_i in its ATPase protective effect was studied. Arsenate (almost as efficient as P_i) and sulfate (less efficiently) were able to protect the enzyme activity (Figure 4), whereas acetate (10 mM) was ineffective.

Sulfate was shown to compete with P_i when the rates of respiration-supported ATP synthesis were measured at saturating ADP concentrations. The apparent K_m for P_i and the K_i for sulfate were 150 and 180 μM, respectively, if estimated assuming a simple competitive type of inhibition (results not shown). Although competition between P_i and sulfate in oxidative phosphorylation was evident, the double-reciprocal plots obtained in the presence of sulfate deviated from a straight line in the high concentration range. This phenomenon was not further studied.

The most likely reason for the deactivation of ATPase in the absence of added P_i during turnover as shown in Figure 1 seemed to originate from the widely studied although not completely understood so-called ADP(Mg^{2+})-induced inhibition, the phenomenon characteristic of all F_1-type ATPases studied so far (*62*). In particular, latent PF_o·F_1 ATPase was shown to be kinetically equivalent to the azide-trapped, ADP-(Mg^{2+})-inhibited MF_o·F_1 (*18*). Although P_i was unable to reactivate ATPase in the absence of pmf (Figure 2), we reasoned that activating anions (P_i and sulfate) should, at least partially, prevent the "spontaneous" (in fact, ADP reassociation-induced) transformation of active ATPase into its latent form. The results presented in Figure 5 show that this was, indeed, the case. Both P_i and SO_4 delayed deactivation caused by elimination of pmf.

DISCUSSION

Numerous stable enzyme−substrate (products) complexes are expected to exist when F_o·F_1 catalyzes the steady-state ATP hydrolysis or (and) synthesis. At least five different forms of an ATPase having a single catalytic site [empty and ATP-, (ADP+P_i)-, ADP-, and P_i-loaded] are anticipated

at any given concentration of the substrate and products. This number becomes as large as 35 for F_1-type ATPases (tree catalytic sites), assuming that bindings of ATP and P_i at a single catalytic site are mutually exclusive. What particular complexes are kinetically significant during the steady-state ATP hydrolysis and/or pmf-supported ATP synthesis remains to be established.

We showed here, for the first time, the significant effect of P_i at low physiologically relevant concentrations (comparable with its apparent K_m in oxidative phosphorylation) on the steady-state coupled ATPase activity. P_i drastically increases the steady-state ATPase activity catalyzed by pmf-induced ATPase with no effects on the "initial" rates (Figure 1). The time-dependent decrease in the rate of the ATPase reaction catalyzed by $MF_o{\cdot}F_1$ was shown to be a consequence of the turnover-dependent formation of the ADP(Mg^{2+})-inhibited enzyme (*62*). The findings that P_i protects $PF_o{\cdot}F_1$ ATPase against spontaneous deactivation (Figure 5) and that this deactivation is, in fact, caused by the rebinding of ADP which dissociates during pmf-induced activation (*18*) suggest that the ADP(Mg^{2+})-inhibited form of the enzyme is the key intermediate responsible for the effect of P_i on the steady-state ATP hydrolysis.

The kinetic scheme that consistently explains the findings reported in this paper is depicted in Figure 6.

We propose that the major pathway of coupled proton-translocating ATP hydrolysis (when pmf is present) proceeds via steps 1−4 and P_i irreversibly leaves the enzyme after ADP dissociation. Essentially irreversible step 4 is likely to be the "stroke" step which is coupled with proton translocation. A predominance of steps 3 and 4 over steps 5 and 6 during coupled steady-state catalysis is presumably due to the inability of P_i to dissociate from the E·(D+P_i) complex (energy-dependent tight binding of P_i to the E·D complex). P_i rapidly and irreversibly dissociates (step 5) when the pmf decreases, thus leaving the E·D complex which then isomerizes into the dead-end E*·D complex [step 7, formation of the ADP(Mg^{2+})-inhibited enzyme]. The reaction pathway via steps 1, 2, 5, and 6 operates when uncoupled $F_o{\cdot}F_1$ or the soluble F_1 catalyzes ATP hydrolysis. When pmf-induced, pmf-generating ATP hydrolysis proceeds in the presence of arsenate or sulfate (Figure 4), the ternary E·(D+As) or E·(D+SO_4) complexes are formed, thus protecting the enzyme from isomerization into the dead-end ADP(Mg^{2+})-inhibited species. We believe that the kinetic scheme shown in Figure 6 is qualitatively valid for all $F_o{\cdot}F_1$-type ATPases. The differences in the kinetics of $MF_o{\cdot}F_1$, prokaryotic $F_o{\cdot}F_1$, and $CF_o{\cdot}F_1$ ATPase activity seem likely to be quantitative rather than qualitative; the relative affinities of ADP and P_i for the catalytic sites of F_1 ATPases and the rate constants for individual steps are evidently variable among the species.

P_i does not inhibit coupled (this paper) or uncoupled (*50*) ATP hydrolysis catalyzed by F_1-type ATPases. This phenomenon is hard, if not impossible, to explain if any reversibly operating ATPase/synthase model to be considered taking into account the fact that P_i is the substrate of pmf-driven ATP synthesis with an apparent K_m in the millimolar range (see the introductory section).

It seems unlikely that the reversal of steps 6, 5 (energy-dependent tight P_i binding), 2, and 1 is the reaction pathway during ATP synthesis. The evidence for random kinetics of

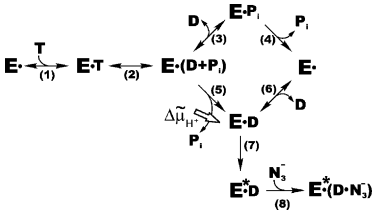

FIGURE 6: Kinetic scheme describing two reaction pathways for coupled and uncoupled ATP hydrolysis catalyzed by pmf-activated $PF_o{\cdot}F_1$ ATPase. T and D stand for ATP and ADP, respectively. The scheme does not attempt to assign individual kinetically distinct steps to the structural rearrangements of the enzyme during the catalysis such as the conformational change within the catalytic sites (open, closed, and half-closed conformations) and the particular position of the γ-subunit relative to the α-subunit−β-subunit interface nucleotide-binding sites. For the sake of simplicity, the enzyme is shown as a single catalytic unit and occupation of three (*63*) or two (*64*) catalytically competent sites by ATP, ADP, and P_i at each step is not specified. For example, one β-subunit may participate in step 1, whereas another β-subunit may catalyze the chemical transformation depicted as step 2 (binding change mechanism) (*7*). The participation of Mg^{2+} as nucleotide−Mg^{2+} complexes and free cations is also not specified. Steps 1−6 are the catalytic turnover steps. Step 5 likely corresponds to the release of P_i during unisite catalysis by mutated TF_1 accompanied by the conformational change in the β-subunit (*65*). The dead-end ADP-(Mg^{2+})-inhibited form (latent $PF_o{\cdot}F_1$ ATPase) is marked with an asterisk. This form is apparently intrinsically very stable in $PF_o{\cdot}F_1$ and additionally stabilized in $MF_o{\cdot}F_1$ if azide is present (step 8). An azide anion ($pK_a = 4.7$) may occupy a P_i-binding site, thus producing an E*·(ADP+N_3^-) complex (*66*) structurally analogous to the enzyme−tightly bound ATP complex or ADP·aluminum·fluoride (*5*) or ADP·V_i·fluoride (*67*) complexes. Slow (compared to the catalytic turnover) isomerization of the E·D intermediate into the dead-end ADP(Mg^{2+})-inhibited form is shown as step 7. Step 5 is shown as pmf-dependent P_i binding and/or dissociation; i.e., P_i binds tightly or dissociates irreversibly when the coupling membrane is energized or de-energized, respectively. "Reversible" and "irreversible" steps are indicated by double-headed and single-headed arrows, respectively. The term irreversible is used solely to indicate that no binding of a particular ligand occurs at physiologically relevant concentrations. The scheme is an extension of the originally proposed kinetic mechanism of uncoupled ATP hydrolysis catalyzed by F_1-type ATPase (*62*, *68*) as adapted for the more physiologically relevant proton translocation-coupled reaction.

ATP synthesis catalyzed by $PF_o{\cdot}F_1$, the same species that used in these studies, has been presented (*39*). The dead-end ADP(Mg^{2+})-inhibited form, which is stabilized by azide in $MF_o{\cdot}F_1$ (*68*) or intrinsically stable in $PF_o{\cdot}F_1$ (*18*), is an unlikely intermediate of ATP synthesis because the latter process is azide-insensitive (*12*, *14*) and, more significantly, the mutated TF_1 incapable of ATP-promoted activation of the inhibited form is fully active in the ATP synthase reaction (*14*). The apparent affinity of P_i for the energized $PF_o{\cdot}F_1$ is much higher [$K_{0.5} = 8-15$ μM (this paper)] than the apparent K_m for P_i in the ATP synthesis reaction (this paper and ref *38*). Taken together, these facts agree with the proposal that different states (conformations) of $F_o{\cdot}F_1$ catalyze pmf-generating ATPase or pmf-driven ATP synthase reactions (*12*−*16*). Further detailed kinetic studies of $F_o{\cdot}F_1$ operating in the ATP synthase mode, particularly with respect to the order of the substrates binding to the enzyme, are required to determine whether the intermediates of uncoupled or coupled ATP hydrolysis catalyzed by F_1 are different from those which exist during coupled ATP synthesis. The molecular mechanism for the ATPase−ATP synthase switch remains unclear. A likely candidate is the ϵ-subunit for which

two dramatically different structures have been established (*69*, *70*). The specific binding of ATP to the ϵ-subunit accompanied by its up and down conformational change has been suggested to serve as the physiologically important ATP-sensing mechanism (*71*). The kinetic scheme shown in Figure 6 attempts to interpret the findings reported in this paper with minimal assumptions. At present, more complex models, such as the possibility of the specific pmf-sensitive P_i binding at the site separated from the β-subunit-located catalytic sites (ϵ-subunit?), cannot be excluded.

ACKNOWLEDGMENT

We thank Dr. E. V. Gavrikova for her great help in preparation of tightly coupled *P. denitrificans* vesicles.

REFERENCES

1. Abrahams, J. P., Leslie, A. G., Lutter, R., and Walker, J. E. (1994) Structure at 2.8 Å resolution of F_1-ATPase from bovine heart mitochondria, *Nature 370*, 621−628.
2. Bianchet, M. A., Hullihen, J., Pedersen, P. L., and Amzel, L. M. (1998) The 2.8-Å structure of rat liver F_1-ATPase: Configuration of a critical intermediate in ATP synthesis/hydrolysis, *Proc. Natl. Acad. Sci. U.S.A. 95*, 11065−11070.
3. Shirakihara, Y., Leslie, A. G., Abrahams, J. P., Walker, J. E., Ueda, T., Sekimoto, Y., Kambara, M., Saika, K., Kagawa, Y., and Yoshida, M. (1997) The crystal structure of the nucleotide-free $\alpha_3\beta_3$ subcomplex of F_1-ATPase from the thermophilic *Bacillus* PS3 is a symmetric trimer, *Structure 15*, 825−836.
4. Groth, G., and Pohl, E. (2001) The structure of the chloroplast F_1-ATPase at 3.2 Å resolution, *J. Biol. Chem. 276*, 1345−1352.
5. Menz, R. I., Walker, J. E., and Leslie, A. G. (2001) Structure of bovine mitochondrial F_1-ATPase with nucleotide bound to all three catalytic sites: Implications for the mechanism of rotary catalysis, *Cell 106*, 331−341.
6. Kagawa, R., Montgomery, M. G., Braig, K., Leslie, A. G., and Walker, J. E. (2004) The structure of bovine F_1-ATPase inhibited by ADP and beryllium fluoride, *EMBO J. 23*, 2734−2744.
7. Boyer, P. D. (1993) The binding change mechanism for ATP synthase: Some probabilities and possibilities, *Biochim. Biophys. Acta 1140*, 215−250.
8. Boyer, P. D. (2001) Toward an adequate scheme for the ATP synthase catalysis, *Biochemistry (Moscow) 66*, 1058−1066.
9. Junge, W., Sabbert, D., and Engelbrecht, S. (1996) ATP-synthesis. Rotary catalysis by F-ATPase: Real-time recording of intersubunit rotation, *Ber. Bunsen-Ges. 100*, 2014−2019.
10. Noji, H., Yasuda, R., Yoshida, M., and Kinosita, K., Jr. (1997) Direct observation of the rotation of F_1-ATPase, *Nature 386*, 299−302.
11. Vinogradov, A. D. (2000) Steady-state and pre-steady-state kinetics of the mitochondrial F_1F_o ATPase: Is ATP synthase a reversible molecular machine? *J. Exp. Biol. 203*, 41−49.
12. Syroeshkin, A. V., Vasilyeva, E. A., and Vinogradov, A. D. (1995) ATP synthesis catalyzed by the mitochondrial F_1F_o ATP synthase is not a reversal of its ATPase activity, *FEBS Lett. 366*, 29−32.
13. Minkov, I. B., Vasilyeva, E. A., Fitin, A. F., and Vinogradov, A. D. (1980) Differential effects of ADP on ATPase and oxidative phosphorylation in submitochondrial particles, *Biochem. Int. 1*, 478−485.
14. Bald, D., Amano, T., Muneyuki, E., Pitard, B., Rigaud, J. L., Kruip, J., Hisabori, T., Yoshida, M., and Shibata, M. (1998) ATP synthesis by F_oF_1-ATP synthase independent of noncatalytic nucleotide binding sites and insensitive to azide inhibition, *J. Biol. Chem. 273*, 865−870.
15. Tsunoda, S. P., Rodgers, A. J., Aggeler, R., Wilce, M. C., Yoshida, M., and Capaldi, R. A. (2001) Large conformational changes of the ϵ subunit in the bacterial F_1F_o ATP synthase provide a ratchet action to regulate this rotary motor enzyme, *Proc. Natl. Acad. Sci. U.S.A. 98*, 6560−6564.
16. Suzuki, T., Murakami, T., Iino, R., Suzuki, J., Ono, S., Shirakihara, Y., and Yoshida, M. (2003) F_oF_1-ATPase/synthase is geared to the synthesis mode by conformational rearrangement of ϵ subunit in response to proton motive force and ADP/ATP balance, *J. Biol. Chem. 278*, 46840−46846.
17. Hyndman, D. J., Milgrom, Y. M., Bramhall, E. A., and Cross, R. L. (1994) Nucleotide-binding sites on *Escherichia coli* F_1-ATPase. Specificity of noncatalytic sites and inhibition at catalytic sites by MgADP, *J. Biol. Chem. 269*, 28871−28877.
18. Zharova, T. V., and Vinogradov, A. D. (2004) Energy-dependent transformation of F_o·F_1-ATPase in *Paracoccus denitrificans* plasma membranes, *J. Biol. Chem. 279*, 2319−2324.
19. Penefsky, H. S. (1977) Reversible binding of P_i by beef heart mitochondrial adenosine triphosphatase, *J. Biol. Chem. 252*, 2891−2899.
20. Kasahara, M., and Penefsky, H. S. (1978) High affinity binding of monovalent P_i by beef heart mitochondrial adenosine triphosphatase, *J. Biol. Chem. 253*, 4180−4187.
21. Penefsky, H. S. (2005) P_i binding by the F_1-ATPase of beef heart mitochondria and of the *Escherichia coli* plasma membrane, *FEBS Lett. 579*, 2250−2252.
22. Kozlov, I. A., and Vulfson, E. N. (1985) Tightly bound nucleotides affect phosphate binding to mitochondrial F_1-ATPase, *FEBS Lett. 182*, 425−428.
23. Hutton, R. L., and Boyer, P. D. (1979) Subunit interaction during catalysis. Alternating site cooperativity of mitochondrial adenosine triphosphatase, *J. Biol. Chem. 254*, 9990−9999.
24. Grubmeyer, C., Cross, R. L., and Penefsky, H. S. (1982) Mechanism of ATP hydrolysis by beef heart mitochondrial ATPase. Rate constants for elementary steps in catalysis at a single site, *J. Biol. Chem. 257*, 12092−12100.
25. Cunningham, D., and Cross, R. L. (1988) Catalytic site occupancy during ATP hydrolysis by MF_1-ATPase. Evidence for alternating high affinity sites during steady-state turnover, *J. Biol. Chem. 263*, 18850−18856.
26. Penefsky, H. S. (1985) Reaction mechanism of the membrane-bound ATPase of submitochondrial particles from beef heart, *J. Biol. Chem. 260*, 13728−13734.
27. Schatz, G., and Racker, E. (1966) Partial resolution of the enzymes catalyzing oxidative phosphorylation. VII. Oxidative phosphorylation in the diphosphopyridine nucleotide-cytochrome b segment of the respiratory chain: Assay and properties in submitochondrial particles, *J. Biol. Chem. 241*, 1429−1438.
28. Ernster, L., Lee, C.-P., and Janda, S. (1967) The reaction sequence in oxidative phosphorylation, in *Biochemistry of mitochondria* (Slater, E. C., Kaniuga, Z., and Wojtczak, L., Eds.) pp 29−51, Academic Press, London.
29. Kayalar, C., Rosing, J., and Boyer, P. D. (1976) 2,4-Dinitrophenol causes a marked increase in the apparent K_m of P_i and of ADP for oxidative phosphorylation, *Biochem. Biophys. Res. Commun. 72*, 1153−1159.
30. Hatefi, Y., Yagi, T., Phelps, D. C., Wong, S. Y., Vik, S. B., and Galante, Y. M. (1982) Substrate binding affinity changes in mitochondrial energy-linked reactions, *Proc. Natl. Acad. Sci. U.S.A. 79*, 1756−1760.
31. Schuster, S. M., Reinhart, G. D., and Lardy, H. A. (1977) Studies on the kinetic mechanism of oxidative phosphorylation, *J. Biol. Chem. 252*, 427−432.
32. Etzold, C., Deckers-Hebestreit, G., and Altendorf, K. (1997) Turnover number of *Escherichia coli* F_oF_1 ATP synthase for ATP synthesis in membrane vesicles, *Eur. J. Biochem. 243*, 336−343.
33. Al-Shawi, M. K., Ketchum, C. J., and Nakamoto, R. K. (1997) The *Escherichia coli* F_oF_1 γ M23K uncoupling mutant has a higher $K_{0.5}$ for P_i. Transition state analysis of this mutant and others reveals that synthesis and hydrolysis utilize the same kinetic pathway, *Biochemistry 36*, 12961−12969.
34. Tomashek, J. J., Glagoleva, O. B., and Brusilow, W. S. (2004) The *Escherichia coli* F_1F_o ATP synthase displays biphasic synthesis kinetics, *J. Biol. Chem. 279*, 4465−4470.
35. Richard, P., Pitard, B., and Rigaud, J. L. (1995) ATP synthesis by the F_oF_1-ATPase from the thermophilic *Bacillus* PS3 co-reconstituted with bacteriorhodopsin into liposomes. Evidence for stimulation of ATP synthesis by ATP bound to a noncatalytic binding site, *J. Biol. Chem. 270*, 21571−21578.
36. Junge, W. (1987) Complete tracking of transient proton flow through active chloroplast ATP synthase, *Proc. Natl. Acad. Sci. U.S.A. 84*, 7084−7088.
37. McCarthy, J. E., and Ferguson, S. J. (1983) The effects of partial uncoupling upon the kinetics of ATP synthesis by vesicles from *Paracoccus denitrificans* and by bovine heart submitochondrial particles. Implications for the mechanism of the proton-translocating ATP synthase, *Eur. J. Biochem. 132*, 425−431.
38. Perez, J. A., and Ferguson, S. J. (1990) Kinetics of oxidative phosphorylation in *Paracoccus denitrificans*. 1. Mechanism of

ATP synthesis at the active site(s) of F_oF_1-ATPase, *Biochemistry 29*, 10503−10518.
39. Perez, J. A., and Ferguson, S. J. (1990) Kinetics of oxidative phosphorylation in *Paracoccus denitrificans.* 2. Evidence for a kinetic and thermodynamic modulation of F_oF_1-ATPase by the activity of the respiratory chain, *Biochemistry 29*, 10518−10526.
40. Selman, B. R., and Selman-Reimer, S. (1981) The steady state kinetics of photophosphorylation, *J. Biol. Chem. 256*, 1722−1726.
41. Kayalar, C., Rosing, J., and Boyer, P. D. (1977) An alternating site sequence for oxidative phosphorylation suggested by measurement of substrate binding patterns and exchange reaction inhibitions, *J. Biol. Chem. 252*, 2486−2491.
42. Rosing, J., Kayalar, C., and Boyer, P. D. (1977) Evidence for energy-dependent change in phosphate binding for mitochondrial oxidative phosphorylation based on measurements of medium and intermediate phosphate-water exchanges, *J. Biol. Chem. 252*, 2478−2485.
43. Feldman, R. I., and Sigman, D. S. (1982) The synthesis of enzyme-bound ATP by soluble chloroplast coupling factor 1, *J. Biol. Chem. 257*, 1676−1683.
44. Feldman, R. I., and Sigman, D. S. (1983) The synthesis of ATP by the membrane-bound ATP synthase complex from medium $^{32}P_i$ under completely uncoupled conditions, *J. Biol. Chem. 258*, 12178−12183.
45. Sakamoto, J. (1984) Effect of dimethylsulfoxide on ATP synthesis by mitochondrial soluble F_1-ATPase, *J. Biochem. 96*, 483−477.
46. Yohda, M., Kagawa, Y., and Yoshida, M. (1986) The synthesis of enzyme-bound ATP by the F_1-ATPase from the thermophilic bacterium PS3 in the presence of organic solvents, *Biochim. Biophys. Acta 850*, 429−435.
47. Bertina, R. M., and Slater, E. C. (1975) The effects of phosphate and electron transport on the carbonyl cyanide *m*-chlorophenylhydrazone-induced ATPase of rat-liver mitochondria, *Biochim. Biophys. Acta 376*, 492−504.
48. Mitchell, P., and Moyle, J. (1971) Activation and inhibition of mitochondrial adenosine triphosphatase by various anions and other agents, *Bioenergetics 2*, 1−11.
49. Moyle, J., and Mitchell, P. (1975) Active/inactive state transitions of mitochondrial ATPase molecules influenced by Mg^{2+}, anions and aurovertin, *FEBS Lett. 56*, 55−61.
50. Yalamova, M. V., Vasilyeva, E. A., and Vinogradov, A. D. (1982) Mutually dependent influence of ADP and P_i on the activity of mitochondrial adenosine triphosphatase, *Biochem. Int. 4*, 337−344.
51. Bulygin, V. V., and Vinogradov, A. D. (1991) Interaction of Mg^{2+} with F_oF_1 mitochondrial ATPase as related to its slow active/inactive transition, *Biochem. J. 276*, 149−156.
52. Matsui, T., Muneyuki, E., Honda, M., Allison, W. S., Dou, C., and Yoshida, M. (1997) Catalytic activity of the $\alpha_3\beta_3\gamma$ complex of F_1-ATPase without noncatalytic nucleotide binding site, *J. Biol. Chem. 272*, 8215−8221.
53. Bald, D., Muneyuki, E., Amano, T., Kruip, J., Hisabori, T., and Yoshida, M. (1999) The noncatalytic site-deficient $\alpha_3\beta_3\gamma$ subcomplex and F_oF_1-ATP synthase can continuously catalyse ATP hydrolysis when P_i is present, *Eur. J. Biochem. 262*, 563−568.
54. Mendel-Hartvig, J., and Capaldi, R. A. (1991) Catalytic site nucleotide and inorganic phosphate dependence of the conformation of the ϵ subunit in *Escherichia coli* adenosinetriphosphatase, *Biochemistry 30*, 1278−1284.
55. Perez, J. A., Greenfield, A. J., Sutton, R., and Ferguson, S. J. (1986) Characterisation of phosphate binding to mitochondrial and bacterial membrane-bound ATP synthase by studies of inhibition with 4-chloro-7-nitrobenzofurazan, *FEBS Lett. 198*, 113−118.
56. Turina, P., Giovannini, D., Gubellini, F., and Melandri, B. A. (2004) Physiological ligands ADP and P_i modulate the degree of intrinsic coupling in the ATP synthase of the photosynthetic bacterium *Rhodobacter capsulatus*, *Biochemistry 43*, 11126−11134.
57. Zharova, T. V., and Vinogradov, A. D. (2003) Proton-translocating ATP-synthase of *Paracoccus denitrificans*: ATP-hydrolytic activity, *Biochemistry (Moscow) 68*, 1101−1118.
58. John, P., and Whatley, F. R. (1970) Oxidative phosphorylation coupled to oxygen uptake and nitrate reduction in *Micrococcus denitrificans*, *Biochim. Biophys. Acta 216*, 342−352.
59. Chance, B., and Nishimura, M. (1967) Sensitive measurements of changes of hydrogen ion concentration, *Methods Enzymol. 10*, 641−650.
60. Hers, H., and van Hof, F. (1966) Enzymes of glycogen degradation in biopsy material, *Methods Enzymol. 8*, 525−532.
61. Kell, D. B., John, P., and Ferguson, S. J. (1978) The protonmotive force in phosphorylating membrane vesicles from *Paracoccus denitrificans*. Magnitude, sites of generation and comparison with the phosphorylation potential, *Biochem. J. 174*, 257−266.
62. Vasilyeva, E. A., Minkov, I. B., Fitin, A. F., and Vinogradov, A. D. (1982) Kinetic mechanism of mitochondrial adenosine triphosphatase. ADP-specific inhibition as revealed by the steady-state kinetics, *Biochem. J. 202*, 9−14.
63. Weber, J., and Senior, A. E. (2001) Bi-site catalysis in F_1-ATPase: Does it exist? *J. Biol. Chem. 276*, 35422−35428.
64. Milgrom, Y. M., and Cross, R. L. (2005) Rapid hydrolysis of ATP by mitochondrial F_1-ATPase correlates with the filling of the second of three catalytic sites, *Proc. Natl. Acad. Sci. U.S.A. 102*, 13831−13836.
65. Masaike, T., Muneyuki, E., Noji, H., Kinosita, K., Jr., and Yoshida, M. (2002) F_1-ATPase changes its conformations upon phosphate release, *J. Biol. Chem. 277*, 21643−21649.
66. Bowler, M. W., Montgomery, M. G., Leslie, A. G., and Walker, J. E. (2006) How azide inhibits ATP hydrolysis by the F-ATPases, *Proc. Natl. Acad. Sci. U.S.A. 103*, 8646−8649.
67. Chen, C., Saxena, A. K., Simcoke, W. N., Garboczi, D. N., Pedersen, P. L., and Ko, Y. H. (2006) Mitochondrial ATP synthase. Crystal structure of the catalytic F_1 unit in a vanadate-induced transition-like state and implications for mechanism, *J. Biol. Chem. 281*, 13777−13783.
68. Vasilyeva, E. A., Minkov, I. B., Fitin, A. F., and Vinogradov, A. D. (1982) Kinetic mechanism of mitochondrial adenosine triphosphatase. Inhibition by azide and activation by sulphite, *Biochem. J. 202*, 15−23.
69. Rodgers, A. J., and Wilce, M. C. (2000) Structure of the γ-ϵ complex of ATP synthase, *Nat. Struct. Biol. 7*, 1051−1054.
70. Gibbons, C., Montgomery, M. G., Leslie, A. G. W., and Walker, J. E. (2000) The structure of the central stalk in bovine F_1-ATPase at 2.4 Å resolution, *Nat. Struct. Biol. 7*, 1055−1061.
71. Iino, R., Murakami, T., Iizuka, S., Kato-Yamada, Y., Suzuki, T., and Yoshida, M. (2005) Real-time monitoring of conformational dynamics of the ϵ subunit in F_1-ATPase, *J. Biol. Chem. 280*, 40130−40134.

BI061520V